Magnetic and atomic short-range order in Cu-rich Cu-Mn

B. Schönfeld,[1] R. Bucher,[1,*] G. Kostorz,[1] and M. Zolliker[2]
[1]*ETH Zürich, Institute of Applied Physics, CH-8093 Zürich, Switzerland*
[2]*Laboratory for Neutron Scattering and PSI, ETH Zürich, CH-5232 Villigen, Switzerland*
(Received 23 November 2003; revised manuscript received 22 March 2004; published 16 June 2004)

Elastic diffuse neutron scattering from Cu-17 at.% Mn was measured within three planes of reciprocal space, at room temperature and at 11 K (far above and below the spin-glass temperature of 71 K) to determine the atomic and magnetic short-range order parameters. Using two samples with frozen-in states of thermal equilibrium of 483 and 553 K, respectively, the antiferromagnetic character of the spin glass was found to be robust against changes in the degree of atomic order while the ferromagnetic character is rapidly reduced with lower atomic order. This confirms conclusions of *ab initio* calculations by Ling *et al.* [J. Phys.: Condens. Matter **6**, 6001 (1994)].

DOI: 10.1103/PhysRevB.69.224205 PACS number(s): 75.50.Lk, 61.66.Dk, 64.90.+b

I. INTRODUCTION

Atomic and magnetic short-range order has been repeatedly investigated in Cu-rich Cu-Mn. For Mn contents of less than 25 at.%, detailed diffuse wide-angle scattering experiments were reported by Wells and Smith[1] [with 15 and 25 at.% Mn, quenched from the γ phase, the magnitude of the scattering vector $h>3$ reciprocal lattice units (r.l.u.)], Hirabayashi *et al.*[2] (with 25 at.% Mn, slowly cooled from 523 to 423 K, $h>2$ r.l.u.], Cable *et al.*[3] (with 25 at.% Mn, slowly cooled from 673 to 463 K and further aged at 373 K, $h>0.1$ r.l.u.), Roelofs *et al.*[4] (with 17.2 at.% Mn, quenched from 483 K, $h>0.15$ r.l.u.), and Osaka and Takama[5] (with 24.3 at.% Mn, quenched from 770 K, $h>3.5$ r.l.u.). The differences in the heat treatments and in the ranges of scattering vectors investigated led to large differences for the value of the diffuse maxima (the degree of local order) or even to a change of the character of order (local order or local decomposition).

At room temperature (RT), elastic diffuse neutron scattering is essentially due to atomic short-range order. Apart from the rapid decrease of the magnetic scattering factor with increasing scattering vectors,[1,2] the magnetic short-range order parameter ξ_{000} is also very small far above the spin-glass temperature,[4] as a consequence of the dynamics of the spins.[6] Atomic short-range order for a state of thermal equilibrium can only be established above about 450 K in a reasonable time; the kinetics further depend on the Mn content.[7] A state of thermal equilibrium investigated by Roelofs *et al.*[4] yielded diffuse maxima of atomic short-range order at $1\frac{1}{2}0$ positions (as in the investigations of different states in Refs. 1–3).

In a recent x-ray investigation of Cu-24.3 at.% Mn quenched from 770 K,[5] short-range order scattering was determined by the Borie-Sparks method.[9] Local maxima found for the short-range order scattering close to Bragg reflections indicated local decomposition. In contrast, Cable *et al.*[3] obtained local order and not local decomposition for a sample of comparable composition slowly cooled from about the same temperature. Concerning the study of Osaka and Takama,[5] two comments may be made. (i) The experiment may have suffered from the low scattering contrast with x-rays of Mo $K\alpha$ radiation, especially as positions at large scattering vectors (larger than 3.6 r.l.u.) were measured. Diffuse maxima are also much more clearly visible in the total diffuse scattering of this alloy if the wavelength of the x rays is tuned to the Mn-K edge to enhance the scattering contrast.[10] (ii) The calculated and subtracted thermal diffuse scattering (TDS) in Ref. 5 is based on elastic constants of pure Cu and not of Cu-rich Cu-Mn, an approximation that underestimates the TDS contribution (this was checked by the present authors for Cu-17.2 at.% Mn, where both sets of elastic constants are known). Thus, the elastic coherent scattering intensity will be overestimated especially around the positions of the Bragg reflections. As Huang scattering was not considered in addition, an apparent presence of local decomposition seems plausible.

Magnetic short-range order scattering far below the corresponding spin-glass temperature was investigated in detail within the (001) plane for alloys of three compositions, for Cu-25 at.% Mn at 10 K by Cable *et al.*,[3] for Cu-17 at.% Mn at 15 K by Roelofs *et al.*[8] and Schönfeld *et al.*,[13] and for Cu-5 at.% Mn at 1.5 K by Murani *et al.*[11] It was obtained as the (calculated) difference in the cross sections at two temperatures (far above and below the spin-glass temperature) and directly by a polarization analysis. For the spin-glass temperature as a function of composition, see Gibbs *et al.*[12] Cable *et al.*[3] considered the temperature-difference results to be better for the more dilute alloys and those from polarization analysis better for alloys with a higher Mn fraction. Under the assumption that magnetic scattering is negligible for the (011) plane, a tentative set of Fourier coefficients was given by Roelofs *et al.*[8] This data set, however, may only represent a first approximation, and a three-dimensional investigation is still required.

Though many scattering experiments of Cu-rich Cu-Mn were performed, a three-dimensional investigation of magnetic short-range order is still missing. For such an investigation, wide-angle and small-angle scatterings of the same sample are required. For the present investigation, two samples of very similar composition, but in two different frozen-in states of atomic short-range order, were chosen for wide-angle neutron scattering experiments, as they had al-

ready been investigated by small-angle neutron scattering.[13] This also allows the correlation between atomic and magnetic short-range order of this spin glass to be addressed. In addition, the predictions of a first-principles theory for magnetic and atomic correlations by Ling *et al.*[14] can be checked stating that for an ideal spin glass (an alloy with a statistically uncorrelated atomic arrangement), diffuse maxima in magnetic scattering would be dominant around $1\frac{1}{2}0$ positions (for the atomic correlations, clustering was obtained in this study,[14] in contrast to the majority of experiments).

II. THEORY

The elastic coherent diffuse neutron scattering from a binary (*A*-*B*) face-centered-cubic (fcc) single crystal, including magnetic scattering, can be written as

$$I(\mathbf{h}) = Nc_Ac_B(b_A - b_B)^2[I_{ASRO}(\mathbf{h}) + I_{SE}(\mathbf{h})] + I_{MSRO}(\mathbf{h}), \tag{1}$$

where N is the number of atoms in the beam, c_A and c_B are the atomic fractions, and b_A and b_B are the coherent scattering lengths (for recent reviews, see, e.g., Kostorz[15] and Schönfeld,[16] and references therein). The factor $Nc_Ac_B(b_A - b_B)^2$ is called one Laue unit (L.u.), $I_{ASRO}(\mathbf{h})$ is the atomic short-range order scattering, $I_{SE}(\mathbf{h}) = \mathbf{h}\cdot\mathbf{Q}(\mathbf{h})$ the linear displacement scattering, and $I_{MSRO}(\mathbf{h})$ the magnetic short-range order scattering. Static diplacements beyond first order are neglected because the measurements were not extended to extremely large scattering vectors. The various terms are explicitly given by

$$I_{ASRO}(\mathbf{h}) = \sum_{lmn} \alpha_{lmn} \cos(\pi h_x l)\cos(\pi h_y m)\cos(\pi h_z n), \tag{2}$$

$$Q_x(\mathbf{h}) = \sum_{lmn} \gamma^x_{lmn} \sin(\pi h_x l)\cos(\pi h_y m)\cos(\pi h_z n), \tag{3}$$

$$I_{MSRO}(\mathbf{h}) = \frac{2}{3}Nc_Br_0^2S(S+1)|f_B(\mathbf{h})|^2\sum_{lmn}[c_B + (1-c_B)\alpha_{lmn}]\xi_{lmn} \times\cos(\pi h_x l)\cos(\pi h_y m)\cos(\pi h_z n) \tag{4}$$

[the other components of $\mathbf{Q}(\mathbf{h})$, $Q_y(\mathbf{h})$, and $Q_z(\mathbf{h})$, are obtained by cyclic exchange of the indices x, y, z]. Here, B refers to the atoms carrying the magnetic moments, r_0 is -0.54×10^{-12} cm, S the spin of the B atoms, $f_B(\mathbf{h})$ the magnetic form factor, and $\xi_{lmn} = \langle \mathbf{S}_{000}(0)\cdot\mathbf{S}_{lmn}(t)\rangle$ the spin-spin correlation function for the lmn type of neighbors (l, m, n in units of half the lattice parameter representing the position). The α_{lmn} are the Warren-Cowley short-range order parameters[17] and the γ^i_{lmn}, $i = x,y,z$ the Fourier coefficients of the linear displacement scattering, which are linear combinations of the individual displacements. In contrast to α_{lmn} and γ^i_{lmn}, the ξ_{lmn} are functions of time t because the spins $\mathbf{S}_{lmn}$ fluctuate and do not contribute to true elastic scattering. Values for ξ_{lmn} thus represent an integration over a time interval defined by the energy resolution in the scattering experiment.

III. EXPERIMENTAL

Two single-crystalline Cu-Mn samples were cut by spark erosion from a crystal grown by the Bridgman method. They were cylindrically shaped with the axis close to ⟨111⟩, about 10 mm in height and diameter. Sample 1 with 17.2(2)at.% Mn and sample 2 with 16.6(2)at.% Mn were homogenized at 1123 K and water quenched (the Mn concentrations were determined by x-ray fluorescence and chemical analysis). Sample 1 was then aged at 483 K (for two weeks), sample 2 at 553 K (for two days) and water quenched to establish well-defined states of thermal equilibrium.[7] The samples in these states had previously been investigated by small-angle neutron scattering (SANS) at Risø National Laboratory, Denmark.[13]

Diffuse neutron scattering with nominally zero-energy transfer was performed at the triple-axis spectrometer IN3 at the Institut Laue-Langevin, Grenoble. Incoming neutrons of an energy of 14.7(6)meV were used. Harmonics were suppressed by a filter of pyrolytic graphite, 10 cm in thickness.

For both samples, diffuse scattering was registered in the (001), (011), and (111) planes of reciprocal space at about 1000 positions per plane covering scattering vectors within 0.2 to 2.3 r.l.u. Positions within a distance of 0.2 r.l.u. around Bragg reflections were excluded. The samples were mounted on the cold finger of a CTI cryostat, with the Al window and heat shield more than 9 cm away from the sample to avoid Debye-Scherrer rings from these materials to be registered. Measurements were done at room temperature and between 11 and 15 K (subsequently designated 11 K, where most data where taken). A hollow Cd cylinder, shielding the sample holder and the glue between the sample holder and the sample, was aligned perpendicular to the scattering plane and employed to define the scattering volume. Typical intensities varied between 2000 and 9000 counts per 90 s. The data were corrected for the background and calibrated by comparing then with the incoherent scattering of a vanadium cylinder of similar dimensions mounted as the samples and employing a point-to-point calibration on a coarse grid.

The data were corrected for absorption and multiple scattering as described by Sears[18] using the absorption cross sections of Ref. 19. An overall (static and dynamic) Debye-Waller factor $\exp[-2B(\sin\theta/\lambda)^2]$ with $B = 7.05\times10^{-3}$ nm^2 was used for Cu-Mn at room temperature.[4] For 11 K, this value was estimated to $B = 2.08\times10^{-3}$ nm^2 (assuming that Poisson's ratio in the estimate of the static Debye-Waller factor[20] does not vary with temperature). A value of $B = 4.85\times10^{-3}$ nm^2 was used for vanadium.[21] The coherent scattering lengths $b_{Cu} = 7.718(4)$fm and $b_{Mn} = -3.73(2)$fm and the incoherent scattering cross sections $\sigma^{inc}_{Cu} = 0.55(3)$b, $\sigma^{inc}_{Mn} = 0.40(2)$b, and $\sigma^{inc}_{V} = 5.08(6)$b were taken from Sears.[19]

IV. RESULTS

The calibrated diffuse scattering of Cu-16.6 at.% Mn (without the elastic incoherent scattering) at 11 K and RT is given in Fig. 1 for the (001) plane. In this plane, all the positions of the diffuse maxima of atomic and magnetic

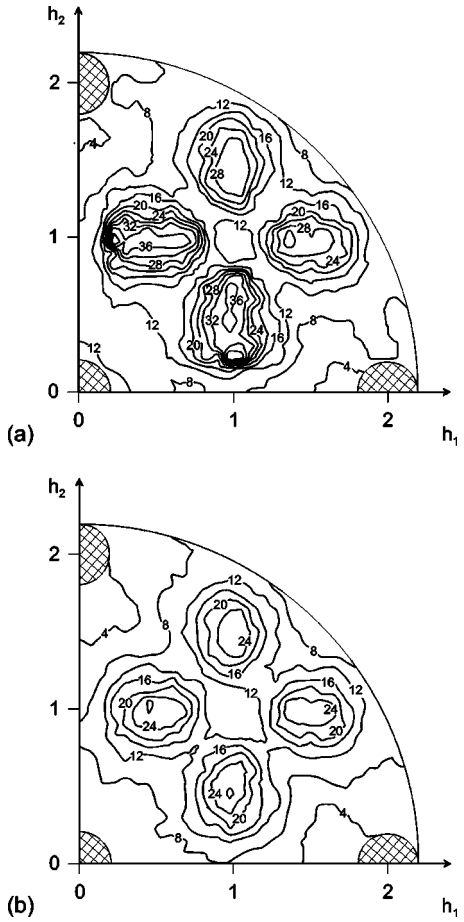

FIG. 1. Elastic coherent neutron scattering of Cu-16.6 at.% Mn in 0.1 Laue units as measured at 11 K (a) and at room temperature (b).

short-range order are located. At both temperatures, the largest scattering intensity is seen near $1\frac{1}{2}0$. While the maximum arises at RT because of atomic short-range order, the larger intensity around $1\frac{1}{2}0$ and the elongation in shape along [010] for the lines of equal intensity at 11 K are due to magnetic short-range order. Within the present instrumental resolution, the $1\frac{1}{2}0$ maximum and the two neighboring $2k_F$ maxima are nearly resolved. The intensity is larger around $1\frac{1}{2}0$ than around $1\frac{3}{2}0$, as the magnetic scattering intensity rapidly decreases with increasing scattering vector. A slight difference in the scattering intensity between $1\frac{1}{2}0$ and $1\frac{3}{2}0$ at RT (also visible in Fig. 3 of Ref. 4 for Cu-17.2 at.% Mn) indicates the presence of magnetic (close to paramagnetic) scattering. At 11 K, the scattering intensity starts to increase towards 000 as the magnetic order of the spin glass also has a ferromagnetic character.

Combining wide-angle scattering with the previously determined small-angle scattering of the same samples,[13] a least-squares fitting analysis was applied. The slight directional dependence in small-angle neutron scattering was discarded (Ref. 22) as it will only affect the Fourier coefficients of the more remote neighbors. The number of Fourier coefficients of atomic short-range order, magnetic short-range order, and linear displacements was chosen according to the variation of the weighted *R*-value of the fit. No adjustment in relative intensities was done, neither between the data of the (001), (011), and (111) planes, nor with the small-angle scattering data. Three data sets were analyzed, those taken at RT and at 11 K, and the calculated difference in scattering at 11 K and RT, allowing the separated contributions to be compared.

(i) At RT, magnetic short-range order scattering (close to paramagnetic scattering) is considered to account for the small-angle scattering found in addition to atomic short-range order scattering and static displacement scattering.

(ii) At 11 K, an unmodified short-range order scattering and a slightly different static displacement scattering (with respect to RT) are present, together with magnetic short-range order scattering characteristic of a state far below the spin-glass temperature.

(iii) The calculated difference of the scattering data at 11 K and RT should correspond to magnetic short-range order scattering (without paramagnetic scattering). It turned out that—probably because of unavoidable though small errors in the calibration and differences in the static displacements at both temperatures—some atomic short-range order scattering and static displacement scattering intensities were still present in the difference and their contribution was considered in the least-squares fitting.

The Fourier coefficients of the various data analyses are summarized in Tables I–III; the recalculated scattering contributions are shown in Figs. 2 and 3.

A. Atomic short-range order scattering

The main feature of atomic short-range order scattering is a maximum at $1\frac{1}{2}0$ with ~3.6 L.u. for Cu-17.2 at.% Mn and with ~2.8 L.u. for Cu-16.6 at.% Mn. The largest difference in the analyses of the data sets at 11 K and at RT is seen close to 000 and equivalent points (Fig. 2). While the 11 K data show a clear increase to ~1.5 L.u. for both samples, only a slight increase close to 000 is obtained in the RT data. Furthermore, an increased magnetic scattering of ~1.4 L.u. is obtained at 000 for both samples at RT. Still, the fitted value of ξ_{000} of both samples is within ±0.1, as expected, far above the spin-glass temperature within the energy resolution of the present neutron scattering experiment.[6] The reason for the difficulty of separating atomic and magnetic short-range order scattering close to 000 is obvious; there is little variation of the squared magnetic scattering factor with the magnitude of the scattering vector. Thus, the two scattering contributions are not distinguishable. An unambiguous separation requires data obtained by small-angle x-ray scattering or small-angle neutron scattering with polarization analysis.

If one takes the peak intensity at $1\frac{1}{2}0$ as a measure for the degree of short-range order, a higher degree is seen for the sample with the lower aging temperature. The dependence on aging temperature is also reflected in the magnitudes of the Warren-Cowley short-range order parameters; they are systematically larger up to shell 431 with the lower aging temperature (Table I). The results of Cu-17.2 at.% Mn may also be compared with the evaluation of the three-

TABLE I. Fitted atomic short-range order parameters α_{lmn} of Cu-16.6 at.% Mn and Cu-17.2 at.% Mn (data taken at RT and at 11 K).

	α_{lmn}(Cu-16.6 at.%Mn)		α_{lmn}(Cu-17.2 at.%Mn)	
lmn	RT	11 K	RT	11 K
000	0.9945(55)	1.0642(63)	0.9655(43)	1.0866(57)
110	−0.0846(15)	−0.0807(18)	−0.0949(11)	−0.0962(15)
200	0.0701(15)	0.0802(17)	0.0855(11)	0.0979(14)
211	0.0350(12)	0.0420(14)	0.0422(9)	0.0506(12)
220	−0.0299(14)	−0.0299(16)	−0.0385(10)	−0.0384(14)
310	−0.0112(8)	−0.0114(10)	−0.0199(5)	−0.0219(7)
222	−0.0370(15)	−0.0402(18)	−0.0532(10)	−0.0563(14)
321	0.0135(6)	0.0161(7)	0.0175(4)	0.0219(5)
400	0.0178(17)	0.0244(18)	0.0364(13)	0.0436(16)
330	−0.0158(11)	−0.0139(12)	−0.0193(8)	−0.0208(12)
411	−0.0033(9)	−0.0021(11)	−0.0061(7)	−0.0054(9)
420	0.0011(7)	0.0016(8)	0.0023(5)	0.0043(7)
233	−0.0008(7)	0.0004(7)	0.0011(5)	0.0022(7)
422	−0.0042(8)	−0.0036(10)	−0.0075(6)	−0.0083(9)
431	0.0024(5)	0.0033(7)	0.0005(4)	0.0029(6)
510	0.0008(7)	0.0004(8)	−0.0031(5)	−0.0036(7)
521	0.0018(5)	0.0027(6)	0.0034(4)	0.0046(5)
440	0.0022(10)	0.0005(11)	−0.0006(8)	−0.0001(11)
433	0.0006(6)	0.0011(7)	−0.0001(5)	0.0018(7)
530	−0.0020(6)	−0.0016(7)	−0.0040(5)	−0.0046(7)
244	−0.0013(6)	−0.0012(7)	−0.0016(4)	−0.0027(6)
600	0.0011(13)	0.0033(16)	0.0073(11)	0.0116(15)
532	0.0001(4)	0.0001(5)	0.0002(4)	0.0005(5)
611	−0.0012(7)	−0.0009(8)	−0.0015(5)	−0.0024(7)
620	0.0015(6)	0.0032(7)	0.0011(5)	0.0034(7)
541	−0.0010(4)	0.0003(5)	−0.0013(4)	−0.0002(5)
622	−0.0010(6)	0.0010(7)	−0.0010(5)	0.0001(7)
631	−0.0002(4)	−0.0005(5)	−0.0013(3)	−0.0013(5)
444	−0.0010(10)	−0.0015(11)	−0.0035(8)	−0.0030(11)
543	−0.0010(4)	−0.0002(4)	−0.0014(3)	−0.0001(4)
550	−0.0011(7)	−0.0015(9)	−0.0006(7)	0.0006(9)
710	0.0005(3)	−0.0004(6)	0.0002(2)	−0.0016(6)
640	0.0024(3)	0.0019(6)	0.0019(2)	0.0025(6)
255	0.0006(3)	−0.0003(6)	0.0005(2)	−0.0001(7)
633	0.0003(3)	−0.0004(6)	−0.0002(2)	−0.0009(6)
721	0.0009(2)	0.0005(5)	0.0011(2)	0.0012(5)
642	−0.0006(2)	−0.0007(4)	0.0006(2)	0.0005(4)
730	0.0005(3)	0.0007(6)	0.0003(2)	−0.0009(6)
651	−0.0002(2)	−0.0006(4)	−0.0009(2)	−0.0019(4)
732	0.0007(2)	0.0009(4)	0.0005(2)	0.0002(4)
800	−0.0019(6)	−0.0021(11)	0.0023(5)	0.0028(11)

dimensional data set of Roelofs *et al.*[4] (Note that the data set of Roelofs *et al.*[8] cited in Table I of Ref. 5 refers to magnetic short-range order and is incorrectly attributed to atomic short-range order. Atomic short-range order data are found in Ref. 4). The two sets of α_{lmn} agree within three standard deviations. Two features of the Warren-Cowley short-range order parameters are important. (i) The closeness of α_{000} to 1 and the close agreement in the evaluation of the data sets at RT and 11 K (Table I) show that atomic short-range order scattering was properly separated at 11 K. (ii) The large positive values of the Warren-Cowley short-range order parameters α_{l00} reveal that chains of Mn atoms along ⟨100⟩

TABLE II. The first 48 fitted magnetic short-range order parameters ξ_{lmn} of Cu-16.6 at.% Mn and Cu-17.2 at.% Mn (data taken at 11 K and calculated difference of the 11 K at RT data) (Ref. 27).

	ξ_{lmn}(Cu-16.6 at.%Mn)		ξ_{lmn}(Cu-17.2 at.%Mn)	
lmn	11 K	11 K – RT	11 K	11 K – RT
000	0.506(20)	0.623(11)	0.626(19)	0.627(11)
110	−0.449(57)	−0.488(31)	−0.612(52)	−0.499(32)
200	0.402(22)	0.419(16)	0.417(18)	0.391(14)
211	0.130(16)	0.200(12)	0.247(18)	0.210(11)
220	−0.048(35)	−0.101(19)	−0.132(31)	−0.075(20)
310	−0.176(17)	−0.174(12)	−0.134(15)	−0.112(11)
222	−0.230(43)	−0.220(28)	−0.287(38)	−0.180(28)
321	0.134(10)	0.108(7)	0.182(8)	0.138(7)
400	0.246(30)	0.176(21)	0.267(26)	0.154(19)
330	−0.158(24)	−0.148(15)	−0.175(23)	−0.157(16)
411	0.080(20)	0.090(12)	0.066(18)	0.091(12)
420	−0.012(14)	−0.062(9)	0.006(12)	−0.039(9)
233	0.051(13)	0.011(8)	0.060(12)	0.022(9)
422	−0.120(19)	−0.098(10)	−0.081(17)	−0.102(10)
431	0.098(12)	0.107(7)	0.115(10)	0.115(7)
510	−0.052(15)	−0.035(9)	−0.037(14)	−0.040(9)
521	0.060(10)	0.028(6)	0.082(9)	0.060(6)
440	−0.034(20)	−0.110(12)	−0.001(20)	−0.039(14)
433	0.049(12)	0.062(7)	0.067(11)	0.073(8)
530	−0.081(13)	−0.068(8)	−0.068(13)	−0.078(9)
244	−0.087(13)	−0.121(6)	−0.073(11)	−0.101(9)
600	0.137(32)	0.143(14)	0.170(30)	0.231(15)
532	0.021(9)	−0.002(3)	0.043(9)	0.032(4)
611	−0.055(16)	−0.054(6)	−0.043(14)	−0.063(7)
620	0.072(13)	0.081(5)	0.102(12)	0.125(5)
541	0.063(10)	0.079(4)	0.092(10)	0.082(4)
622	0.031(14)	0.041(6)	0.001(14)	0.001(7)
631	−0.007(10)	−0.026(4)	−0.002(9)	−0.025(4)
444	−0.044(21)	−0.097(8)	−0.050(21)	−0.069(9)
543	0.033(8)	0.039(3)	0.046(8)	0.043(3)
550	−0.012(18)	−0.058(7)	−0.078(18)	−0.069(8)
710	0.013(12)	−0.009(5)	0.007(12)	−0.035(6)
640	0.026(11)	0.011(5)	0.035(11)	0.048(5)
255	0.018(13)	−0.012(5)	0.013(13)	0.004(6)
633	−0.012(12)	−0.024(4)	0.015(12)	0.006(6)
721	0.007(9)	0.001(4)	0.021(9)	0.025(5)
642	0.002(8)	−0.006(3)	−0.004(8)	−0.006(4)
730	−0.012(12)	0.001(5)	0.002(12)	−0.013(6)
651	−0.008(8)	−0.008(4)	0.013(18)	0.000(4)
732	0.006(7)	0.018(3)	0.031(7)	0.029(4)
800	0.071(23)	0.072(10)	0.049(22)	0.067(11)
455	0.010(5)	0.008(4)	0.018(6)	0.023(5)
741	0.013(4)	0.011(4)	0.007(5)	0.010(5)
811	−0.018(7)	−0.038(5)	−0.024(7)	−0.012(3)
644	0.003(5)	−0.009(4)	0.005(6)	−0.003(3)
820	0.033(5)	0.041(5)	0.043(6)	0.056(5)
653	0.001(3)	−0.001(8)	−0.010(4)	−0.006(3)

TABLE II. (*Continued.*)
Cu-17.2 at.% Mn (data taken at 11 K and calculated difference of the 11 K at RT data) (Ref. 27).

	ξ_{lmn}(Cu-16.6 at.%Mn)		ξ_{lmn}(Cu-17.2 at.%Mn)	
lmn	11 K	11 K – RT	11 K	11 K – RT
660	0.079(8)	0.059(8)	0.101(10)	0.067(9)

(see, e.g., Ref. 23) are the typical local atomic arrangement in short-range ordered Cu-Mn.

B. Magnetic short-range order scattering at 11 K

The separated (fitted and recalculated) magnetic short-range order scattering is characterized by two maxima, at 000 and at $2k_F$ positions (Fig. 3). The intensities were divided by the squared magnetic scattering factor and normalized to Laue units. A magnetic moment of $4\mu_B$ per manganese atom[24,25] and the magnetic form factor according to Shull *et al.*[26] were used. At the $2k_F$ positions, the recalculated intensity amounts to ~3.3 L.u. for Cu-17.2 at.% Mn and to ~2.7 L.u. for Cu-16.6 at.% Mn. The intensity at 000 amounts to 5.8 L.u. for Cu-17.2 at.% Mn and 2.9 L.u. for Cu-16.6 at.% Mn (at 11 K, the peak intensities are always higher by ~1.2 L.u. with the 11 K data set than for the difference of the 11 K and RT data).

A larger number of Fourier coefficients is required for magnetic than for atomic short-range order scattering (Tables I and II); the longer range in the spin-spin correlations reflects the sharper modulation of magnetic scattering. The value of ξ_{000} is smaller than one. Far below the spin-glass temperature, one expects a value of 1 as had been previously reported by Koga *et al.*[28] who analyzed the closely related spin glass Ag-Mn. The reason for this difference is unknown. The values of ξ_{l00} in Table II are large and positive because of the Mn chains along ⟨100⟩ with parallel aligned spins. The ξ_{lmn} are much larger in magnitude than the α_{lmn}. Both parameter sets show the same sign sequence up to shell 411, reflecting the close connection between both scattering contributions, but also demonstrating that the spin-spin correlations are not a mere decoration of atomic short-range order. The spin-spin parameters do not reveal an obvious dependence on the degree of atomic short-range order. Only the larger ferromagnetic order for the alloy with increased atomic order is seen in the larger number of Fourier coefficients and the slight trend to generally more positive values of ξ_{lmn}.

V. DISCUSSION

The Fourier coefficients of the static atomic displacements (Table III) show no obvious dependence on the degree of order and the temperature of the measurement. Of course, they depend on the Warren-Cowley short-range order parameters, in addition to the species-dependent atomic displacements and the coherent scattering lengths (see, e.g., Refs. 15 and 16). But the difference in the degree of order of both samples is too small to be resolved.

In the least-squares fitting to the calculated difference of the 11 K and RT data, the *R*-value of the fit was the largest among the three analyses. The reason is that the difference is taken between two sharply modulated scattering patterns. The procedure to analyze the low-temperature data to determine the magnetic short-range order seems preferable but may fail if the diffuse maxima of magnetic and atomic short-range order coincide.

TABLE III. The first 13 fitted linear displacement parameters γ^x_{lmn} of Cu-16.6 at.% Mn and Cu-17.2 at.% Mn (data taken at RT and at 11 K) (Ref. 27).

	γ^x_{lmn}(Cu-16.6 at.%Mn)		γ^x_{lmn}(Cu-17.2 at.%Mn)	
lmn	RT	11 K	RT	11 K
110	0.0287(4)	0.0286(4)	0.0260(3)	0.0274(4)
200	−0.0179(10)	−0.0169(11)	−0.0166(9)	−0.0181(11)
211	0.0013(4)	0.0001(4)	0.0006(3)	−0.0011(4)
112	0.0022(3)	0.0022(3)	0.0022(3)	0.0013(4)
220	0.0086(5)	0.0087(5)	0.0075(4)	0.0084(5)
310	0.0001(4)	0.0008(5)	0.0007(4)	0.0025(5)
103	0.0008(4)	0.0014(4)	0.0011(3)	0.0014(5)
222	0.0056(4)	0.0062(5)	0.0069(4)	0.0087(5)
321	0.0008(3)	0.0008(4)	0.0002(3)	−0.0005(4)
213	0.0017(3)	0.0018(3)	0.0017(2)	0.0013(3)
132	0.0008(2)	0.0008(2)	0.0002(2)	0.0002(3)
400	−0.0046(11)	−0.0057(12)	−0.0048(9)	−0.0087(11)
330	0.0037(4)	0.0038(4)	0.0032(3)	0.0043(4)

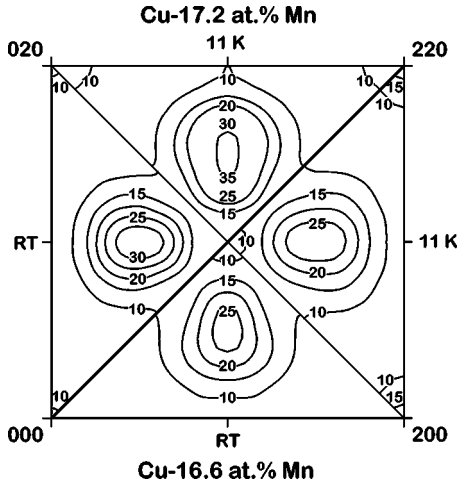

FIG. 2. Atomic short-range order scattering $I_{\mathrm{ASRO}}(\mathbf{h})$ of Cu -16.6 at.% Mn and Cu-17.2 at.% Mn in 0.1 Laue units, as recalculated from the fitted Fourier coefficients of Table I (the data were taken at RT and 11 K). Equidistant lines of equal intensity are shown.

The magnetic scattering of Cu-17 at.% Mn is similar to that of Ag-20.8 at.% Mn (Koga *et al.*,[28] see also Table I of Ref. 8); the spin-spin correlation parameters agree in sign up to shell 600. The major difference in magnetic scattering is seen close to the direct beam where no intensity increase towards the direct beam is found in the recalculated diffuse scattering (Fig. 9 of Koga *et al.*,[28] note that no SANS data were taken). Still, the situation in both alloy systems is quite similar, as the configurational analyses of Ag-Mn and of Cu-Mn give chains of Mn atoms along $\langle 100 \rangle$ as the characteristic feature of the short-range ordered state. For the appearance of magnetic small-angle scattering, the presence of Mn clusters is no prerequisite, as a preferentially parallel alignment of spins on the next-nearest sites will also lead to a scattering enhancement close to the direct beam.

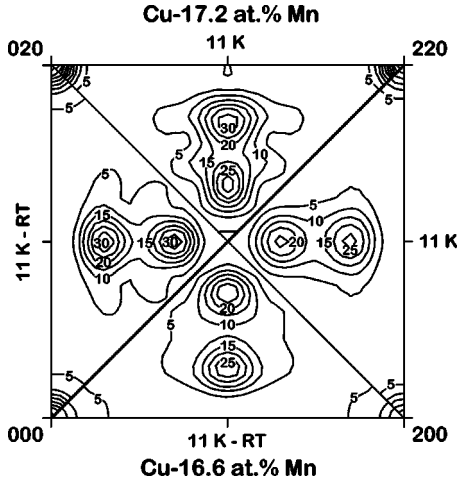

FIG. 3. Magnetic short-range order scattering $I_{\mathrm{MSRO}}(\mathbf{h})/|f_{\mathrm{Mn}}(\mathbf{h})|^2$ of Cu-16.6 at.% Mn and Cu-17.2 at.% Mn in 0.1 Laue units as recalculated from all fitted Fourier coefficients (data taken at 11 K and calculated difference of the data taken at 11 K and RT). Equidistant lines of equal intensity are shown.

The largest difference between the two Cu-Mn samples is found for the peak intensity at 000 below the spin-glass temperature. The intensity decreases by about a factor of 2 with decreasing degree of atomic short-range order, while the intensity at $2k_{\mathrm{F}}$ nearly remains unchanged. More longer Mn chains with the preferentially parallel alignment of spins lead to an increased magnetic scattering near 000. Extrapolating to a statistically uncorrelated arrangement of Cu and Mn atoms, one thus expects a dominance of scattering at $2k_{\mathrm{F}}^{110}$ positions. This compares favorably with the robust location of the maximum in the magnetic short-range order scattering of an alloy with a random atomic arrangement at $1\frac{1}{2}0$ positions and the elongation in shape along [010] (Fig. 1 of Ling *et al.*[14]).

The intensity at 000 far above the spin-glass temperature indicates, in contrast to the calculations of Ling *et al.*,[14] no predominance of decomposition; irrespective of the details of the separation of magnetic and atomic scattering close to 000, the total diffuse scattering is lower than at $1\frac{1}{2}0$. The Cu-Mn alloys are short-range ordered and not short-range decomposed, in contrast to the conclusions of Osaka and Takama.[5]

No long-range ordered state is known experimentally in Cu-rich Cu-Mn. Nevertheless, anomalies in, e.g., electrical resistivity, thermal expansion, or Young's modulus were interpreted as signs of phase transitions (see Gödecke,[29] and references therein). Fast-neutron irradiation at 338 K of a Cu-20 at.% Mn polycrystal led to long-range order in a small fraction of the sample.[30] The order was tentatively described as a $4\times4\times4$ supercell with a slightly tetragonal distortion. No accompanying changes in magnetic scattering were observed,[31] but only wide-angle and no small-angle neutron scattering intensities were taken.

The possible superstructures considered below are all based on $\langle 420 \rangle$ static concentration waves, $D1_{\mathrm{a}}$, $D0_{22}$, and Pt_2Mo.[32] The "NiMo" superstructure would have superstructure peaks exclusively at $1\frac{1}{2}0$ positions and signs of the Warren-Cowley short-range order parameters as those of Table I up to shell 420. However, this structure is not known experimentally.

Preferred long-range ordered structures may be identified by a configurational analysis of modeled short-range ordered crystals. Model crystals (comprising $64\times64\times64$ f.c.c. unit cells) were generated using the Warren-Cowley short-range order parameters of Roelofs *et al.*[4] and analyzed with respect to all 144 nearest-neighbor configurations of the fcc lattice (for the nomenclature of these configurations, see Clapp[33]). Enhancement factors of given configurations were determined by also analyzing crystals of the same composition but with a random arrangement. Table IV shows the configurations with the largest enhancement factors for the case of Mn atoms around Cu atoms. The elements of the superstructures $D1_{\mathrm{a}}$ ($C8$) and $D0_{22}$ ($C16, C17$) repeatedly suggested for Cu-rich Cu-Mn (and also found experimentally in the spin glass Au-Mn), are largely enhanced, but also those of Pt_2Mo ($C38$, found, e.g., in Ni-Cr). A generally excellent agreement is seen with a corresponding configurational analysis of short-range ordered Ni-20.1 at.% Cr (Ref. 34) that also exhibits $1\frac{1}{2}0$ diffuse maxima (Table IV). Any anal-

TABLE IV. Abundance analysis of short-range ordered Cu-17.2 at.% Mn and Ni-20.1 at.% Cr [based on sets of α_{lmn} of Roelofs *et al.* (Ref. 4) and Schönfeld *et al.* (Ref. 34)]. The case of minority atoms around majority atoms is considered. Clapp configurations (Ref. 33) with enhancement factors larger than 3 (with reference to a statistically uncorrelated arrangement) are given.

	Cu-17.2 at.% Mn		Ni-20.1 at.% Cr	
Configuration	Abundance (%)	Enhancement	Abundance (%)	Enhancement
C8	6.6	3.6	6.6	3.2
C16	0.4	9.0	0.5	8.5
C17	1.0	10.1	1.2	9.5
C19	2.5	3.3	3.2	3.1
C35	0.3	3.3	0.5	3.4
C36	0.3	3.3	0.4	3.3
C37	0.3	5.9	0.5	4.2
C38	0.2	5.0	0.3	4.0
C59	0.02	3.5	0.05	3.3
C65	0.06	3.4	0.09	2.9

ogy between Ni_2Cr and Cu_2Mn has to be considered with caution, as spin fluctuations can also affect the atomic order,[14] and they are different in these two alloys.

In conclusion, a detailed investigation of short- and wide-angle neutron scattering is required to obtain relevant data sets of magnetic short-range order. Also, the heat treatment of the spin glass must be well defined, otherwise data sets cannot be compared. This situation strongly resembles the case when atomic short-range order is to be determined; the necessity for following these requirements seems even more stringent for magnetic short-range order studies.

ACKNOWLEDGMENTS

The authors are grateful to E. Fischer for his support in growing the single crystals. This work was partially supported by the "Schweizerische Nationalfonds zur Förderung der wissenschaftlichen Forschung."

*Present address: Department of Physics, University of Cape Town, Rondebosch 7700, South Africa.

[1] W. Wells and J. H. Smith, J. Phys. F: Met. Phys. **1**, 763 (1971).
[2] M. Hirabayashi, M. Koiwa, S. Yamaguchi, and K. Kamata, J. Phys. Soc. Jpn. **45**, 1591 (1978).
[3] J. W. Cable, S. A. Werner, G. P. Felcher, and N. Wakabayashi, Phys. Rev. B **29**, 1268 (1984).
[4] H. Roelofs, B. Schönfeld, G. Kostorz, and W. Bührer, Phys. Status Solidi B **187**, 31 (1995).
[5] K. Osaka and T. Takama, Acta Mater. **50**, 1289 (2002).
[6] H. Pinkvos, A. Kalk, and C. Schwink, Phys. Rev. B **41**, 590 (1990).
[7] R. Reihsner and W. Pfeiler, J. Phys. Chem. Solids **46**, 1431 (1985).
[8] H. Roelofs, B. Schönfeld, G. Kostorz, W. Bührer, J. L. Robertson, P. Zschack, and G. E. Ice, Scr. Mater. **34**, 1393 (1996).
[9] B. Borie and C. J. Sparks, Jr., Acta Crystallogr., Sect. A: Cryst. Phys., Diffr., Theor. Gen. Crystallogr. **27**, 198 (1971).
[10] H. Roelofs, B. Schönfeld, G. Kostorz, J. L. Robertson, P. Zschack, and G. E. Ice (unpublished). The investigations were performed at three photon energies (close to the Mn *K* edge at 6524 eV, close to the Cu *K* edge at 8909 eV, and at 8969 eV) at station X14 at NSLS/Brookhaven.
[11] A. P. Murani, O. Schärpf, K. H. Andersen, D. Richard, and R. Raphel, Physica B **267–268**, 131 (1999).
[12] P. Gibbs, T. M. Harders, and J. H. Smith, J. Phys. F: Met. Phys. **15**, 213 (1985).
[13] B. Schönfeld, O. Paris, G. Kostorz, and J. Skov Pedersen, J. Phys.: Condens. Matter **10**, 8395 (1998).
[14] M. F. Ling, J. B. Staunton, and D. D. Johnson, J. Phys.: Condens. Matter **6**, 6001 (1994).
[15] G. Kostorz, in *Physical Metallurgy*, edited by R. W. Cahn and P. Haasen (North-Holland, Amsterdam, 1996) p. 1115.
[16] B. Schönfeld, Prog. Mater. Sci. **44**, 435 (1999).
[17] J. Cowley, Phys. Rev. **77**, 669 (1950).
[18] V. F. Sears, Adv. Phys. **24**, 1 (1975).
[19] V. F. Sears, Neutron News **3**, 26 (1992).
[20] M. A. Krivoglaz, *X-ray and Neutron Diffraction in Nonideal Crystals* (Springer, Berlin, 1996).
[21] R. Colella and B. W. Batterman, Phys. Rev. B **1**, 3913 (1970).
[22] B. Schönfeld, M. J. Portmann, G. Kostorz, and J. Kohlbrecher, Phys. Rev. B **66**, 100102(R) (2002).
[23] L. Reinhard, B. Schönfeld, G. Kostorz, and W. Bührer, Phys. Rev. B **41**, 1727 (1990).
[24] J. R. Davis, S. K. Burke, and B. D. Rainford, J. Magn. Magn. Mater. **15–18**, 151 (1980).
[25] T. M. Harders, T. J. Hicks, and J. H. Smith, J. Phys. F: Met. Phys. **13**, 1263 (1983).
[26] C. G. Shull, W. A. Strauser, and E. A. Wollan, Phys. Rev. **83**, 333 (1951).

[27] Complete listings are available from the authors. Email address: schoenfeld@iap.phys.ethz.ch (B. Schönfeld).
[28] K. Koga, K.-I. Ohshima, and N. Niimura, Phys. Rev. B **47**, 5783 (1993).
[29] T. Gödecke, Z. Metallkd. **81**, 826 (1990).
[30] L. D. Cussen, E. MacA. Gray, A. P. Murani, S. J. Kennedy, and B. A. Hunter, Europhys. Lett. **58**, 243 (2002).
[31] E. MacA. Gray, L. D. Cussen, A. P. Murani, and S. J. Kennedy, Appl. Phys. A: Mater. Sci. Process. **74**, S935 (2002).
[32] D. de Fontaine, Acta Metall. **23**, 553 (1975).
[33] P. C. Clapp, Phys. Rev. B **4**, 255 (1971).
[34] B. Schönfeld, L. Reinhard, G. Kostorz, and W. Bührer, Phys. Status Solidi B **148**, 457 (1988).